

# Hyperglycemia Mediates a Shift From Cap-Dependent to Cap-Independent Translation Via a 4E-BP1-Dependent Mechanism

Michael D. Dennis,<sup>1</sup> Jeffrey S. Shenberger,<sup>2</sup> Bruce A. Stanley,<sup>3</sup> Scot R. Kimball,<sup>1</sup> and Leonard S. Jefferson<sup>1</sup>

Diabetes and its associated hyperglycemia induce multiple changes in liver function, yet we know little about the role played by translational control of gene expression in mediating the responses to these conditions. Here, we evaluate the hypothesis that hyperglycemia-induced *O*-GlcNAcylation of the translational regulatory protein 4E-BP1 alters hepatic gene expression through a process involving the selection of mRNA for translation. In both streptozotocin (STZ)-treated mice and cells in culture exposed to hyperglycemic conditions, expression of 4E-BP1 and its interaction with the mRNA cap-binding protein eIF4E were enhanced in conjunction with downregulation of cap-dependent and concomitant upregulation of cap-independent mRNA translation, as assessed by a bicistronic luciferase reporter assay. Phlorizin treatment of STZ-treated mice lowered blood glucose concentrations and reduced activity of the cap-independent reporter. Notably, the glucose-induced shift from cap-dependent to cap-independent mRNA translation did not occur in cells lacking 4E-BP1. The extensive nature of this shift in translational control of gene expression was revealed using pulsed stable isotope labeling by amino acids in cell culture to identify proteins that undergo altered rates of synthesis in response to hyperglycemia. Taken together, these data provide evidence for a novel mechanism whereby *O*-GlcNAcylation of 4E-BP1 mediates translational control of hepatic gene expression. *Diabetes* 62:2204–2214, 2013

**R**egulation of gene expression at the level of translation initiation plays a critical role in biological processes such as cellular proliferation, development, and response to biological cues and environmental stresses. Recruitment of ribosomes to mRNA is the rate-limiting step in translation initiation, which in mammalian cells occurs through both cap-dependent and cap-independent mechanisms. According to the traditional model proposed for cap-dependent translation, recruitment of the ribosome onto eukaryotic mRNA occurs upon recognition of the m<sup>7</sup>GTP cap at the 5'-end of mRNA by eIF4F, followed by binding of the eIF4F-mRNA complex to the 40S ribosomal subunit (1). Alternatively, some cellular mRNAs contain unique RNA elements known as internal ribosomal entry sites (IRES)

that enable them to use a cap-independent mechanism of translation initiation (2). An IRES is a highly structured nucleotide sequence located in the 5'-untranslated region (UTR) that promotes binding of 40S ribosomal subunits to a portion of the mRNA at or near the AUG start codon (3). The inclusion of IRES elements in the 5'-UTR of messages allows them to be translated under physiological stress conditions wherein cap-dependent protein synthesis is compromised (4–7).

With the exception of eIF4E, the same canonical initiation factors that facilitate cap-mediated loading of ribosomes onto mRNA are required for cap-independent initiation (8). Further, eIF4E has been shown to function as a negative modulator of IRES-mediated translation by increasing competition from capped mRNAs for initiation factor complexes (9). The interaction of eIF4E and eIF4G is of critical importance for cap-dependent initiation and is principally regulated by eIF4E sequestering proteins, such as 4E-BP1. Binding of 4E-BP1 to eIF4E is mutually exclusive of eIF4E interaction with eIF4G and is controlled by the sequential phosphorylation of serine/threonine residues on 4E-BP1 (10). Hypophosphorylated 4E-BP1 binds eIF4E strongly; however, upon phosphorylation 4E-BP1 releases eIF4E, allowing eIF4E to interact with eIF4G, which promotes ribosome loading onto the mRNA 5'-cap. Thus, conditions that promote 4E-BP1 binding to eIF4E potentially act as a switch between cap-dependent and cap-independent translation. Intriguingly, we have recently showed that under hyperglycemic conditions 4E-BP1 is also modified by addition of *N*-Acetylglucosamine to Ser or Thr residues (*O*-GlcNAcylation), which enhanced its interaction with eIF4E independent of phosphorylation status (11).

Hyperglycemia increases the flux of glucose through the hexosamine biosynthetic pathway (HBP) to increase the production of uridine diphosphate (UDP) *N*-Acetylglucosamine, which promotes protein *O*-GlcNAcylation (12) and contributes to the pathophysiology of diabetes (13). *O*-linked GlcNAcylation has been shown to influence protein function by altering subcellular localization, protein-protein interactions, DNA binding, enzyme activity, and turnover rates (14–18). *O*-GlcNAcylation modification is dynamic, cycling rapidly on and off proteins in a manner that is more reminiscent of protein phosphorylation than other forms of common glycosylation (19). The *O*-GlcNAcylation cycling reactions are catalyzed by the enzymes *O*-GlcNAcylation transferase and *O*-GlcNAcase (20–22), which strongly associate with subpopulations of cytosolic ribosomes, suggesting that they play an important role in regulating mRNA translation (23). In the current study, we evaluated the hypothesis that hyperglycemia causes elevated

From the <sup>1</sup>Department of Cellular and Molecular Physiology, The Pennsylvania State University College of Medicine, Hershey, Pennsylvania; the <sup>2</sup>Department of Pediatrics, The Pennsylvania State University College of Medicine, Hershey, Pennsylvania; and the <sup>3</sup>Department of Microbiology, The Pennsylvania State University College of Medicine, Hershey, Pennsylvania.

Corresponding author: Scot R. Kimball, skimball@psu.edu.

Received 19 October 2012 and accepted 17 February 2013.

DOI: 10.2337/db12-1453

© 2013 by the American Diabetes Association. Readers may use this article as long as the work is properly cited, the use is educational and not for profit, and the work is not altered. See <http://creativecommons.org/licenses/by-nc-nd/3.0/> for details.

*O*-GlcNAcylation of 4E-BP1 and enhanced binding of 4E-BP1 to eIF4E, which in turn causes a shift from cap-dependent to cap-independent mRNA translation. Overall, the results support the conclusion that *O*-GlcNAcylation of 4E-BP1 expression underlies a hyperglycemia-mediated shift in gene expression.

## RESEARCH DESIGN AND METHODS

Male (RFL12xBLK6) F1 mice expressing a bicistronic *Renilla* luciferase (LucR)–fibroblast growth factor (FGF-2) IRES–firefly luciferase (LucF) mRNA were treated with 50 mg/mL streptozotocin (STZ) for 5 days to induce diabetes. RFL12 mice have previously been described (24). Diabetes phenotype was confirmed by blood glucose concentrations >400 mg/dL. Four weeks after STZ treatment, phlorizin was administered subcutaneously twice daily for 7 days (11). Procedures were approved by the Pennsylvania State University College of Medicine Institutional Animal Care and Use Committee. Analysis of protein phosphorylation in liver homogenates and immunoprecipitations was performed as previously described (11). LucR and LucF activity was measured by Dual-Glo Luciferase Assay (Promega).

**Cell culture and transfections.** Primary cultures of hepatocytes were prepared from the liver of RFL12x-BLK6F1 and previously described *Eif4ebp1* or *Eif4ebp2* knockout mice (25) using the Worthington Hepatocyte Isolation System (Worthington Biochemical). Prior to plating, *Eif4ebp1* or *Eif4ebp2* knockout hepatocytes were transfected with a bicistronic reporter plasmid containing the vascular endothelial growth factor (VEGF) IRES using an Amaxa Hepatocyte Nucleofector kit (Lonza). Hepatocytes were seeded onto plates coated with rat tail collagen in Williams E Medium (Gibco) supplemented with 5% FBS (Atlas), 1% penicillin/streptomycin, 1  $\mu$ mol/L DMSO, 4  $\mu$ g/mL insulin, 2 mmol/L GlutaMAX (Gibco), and 15 mmol/L HEPES, pH 7.4. After 6 h, cells were transferred to Williams E Medium supplemented with 0.5% penicillin/streptomycin, 0.1  $\mu$ mol/L DMSO, 1% ITS+ (Gibco), 2 mmol/L GlutaMAX, and 15 mmol/L HEPES, pH 7.4, containing either 11 or 33 mmol/L glucose.

Cultures of wild-type and *Eif4ebp1*;*Eif4ebp2* double knockout mouse embryo fibroblasts (MEFs) were maintained in Dulbecco's modified Eagle's medium lacking sodium pyruvate and containing either 25 or 5 mmol/L glucose plus 20 mmol/L mannitol as an osmotic control supplemented with 10% FBS and 1% penicillin/streptomycin. Transfections were performed using Xtremegene HP (Roche). Where indicated, cells were treated with 3 mmol/L glucosamine (Sigma) or 50 nmol/L thiamet G (Cayman) to enhance protein *O*-GlcNAcylation.

**Pulsed stable isotope labeling by amino acids in cell culture.** Cultures of wild-type MEFs were maintained in Dulbecco's modified Eagle's medium designed for SILAC (Sigma). The medium was supplemented with 105 mg/L L-leucine, 146 mg/L L-lysine-HCl, 84 mg/L L-arginine, 10% dialyzed FBS (Sigma), and 1% penicillin/streptomycin. For the low-glucose condition, MEF cultures were maintained in 5 mmol/L glucose supplemented with 20 mmol/L mannitol and labeled for 6 h in medium supplemented as described above except that lysine was replaced with 4,4,5,5-D<sub>4</sub>-L-lysine and arginine with L-arginine-<sup>13</sup>C<sub>6</sub>. For the high-glucose condition, MEF cultures were maintained in 25 mmol/L glucose supplemented with 3 mmol/L glucosamine and labeled in medium containing L-lysine-<sup>13</sup>C<sub>6</sub><sup>15</sup>N<sub>2</sub> and L-arginine-<sup>13</sup>C<sub>6</sub><sup>15</sup>N<sub>4</sub>. Cells were washed with PBS and harvested in 4% sodium dodecyl sulfate, 0.1 mol/L dithiothreitol, and 0.1 mol/L Tris-HCl pH 7.6. Aliquots of lysates (0.1 mg protein) from low and high glucose-treated cells were combined and prepared using filter-aided sample preparation methods as previously described (26) with the following modifications: washes were with 40% 2,2,2-trifluoroethanol (TFE) and 0.05 mol/L ammonium bicarbonate, pH 8.5; cysteine reduction was with 50 mmol/L tris(2-carboxyethyl)phosphine (TCEP), 40% TFE, and 0.05 mol/L ammonium bicarbonate, pH 8.5; and protein digestion was with endoproteinase LysC, trypsin, and 0.05 mol/L ammonium bicarbonate, pH 8.5.

**Mass spectrometry analysis.** The proteolytic digest was subjected to two-dimensional liquid chromatography–tandem mass spectrometry separation and analysis using an ABSciex 5600 TripleTOF mass spectrometer with a Nanoflow source and ProteinPilot 4.2 Beta analysis software. Initial SCX fractionation was performed as previously described (27,28). Each strong cation exchange (SCX) fraction was dried down and resuspended in 2% (v/v) acetonitrile and 0.1% (v/v) formic acid prior to reverse-phase C18 nanoflow-liquid chromatography separation on a chipPLC Nanoflex system equipped with a trap column (200  $\mu$ m  $\times$  0.5 mm Reprosil-Pur C18-AQ 3  $\mu$ m 120 Å) and a separation column (75  $\mu$ m  $\times$  15 cm Reprosil-Pur C18-AQ 3  $\mu$ m 120 Å), using a 185-min gradient of 0.1% formic acid with increasing percentages of acetonitrile containing 0.1% formic acid, delivered into a 5600 TripleTOF mass spectrometer using a NanoSpray III source (ABSciex) with a 10- $\mu$ m ID nanospray tip (New Objective, Woburn, MA). Combined MS and MS/MS spectra were analyzed by ProteinPilot 4.2 Beta software searched against the

complete Mouse RefSeq database from NCBI (27,303 sequences total, from 4 February 2012, concatenated to a reversed sequence Decoy database derived from the same RefSeq database, plus a list of 389 common laboratory contaminants). Protein identifications were accepted if they had an estimated local false discovery rate of <5%, using the Proteomics System Performance Evaluation Pipeline algorithm to calculate the false discovery rates (29).

**Ingenuity Pathways Analysis.** The raw data obtained from the pulsed stable isotope labeling by amino acids in cell culture (pSILAC) analysis was uploaded and analyzed using proteome software Ingenuity Pathways Analysis (IPA) (www.ingenuity.com). A medium:high (M:H) cutoff of 0.5–1.5 was set to identify proteins whose synthesis rates were differentially regulated.

**Statistical analysis.** The data are expressed as means + SE. Statistical analysis is described in the figure legends.

## RESULTS

**Diabetes promotes cap-independent translation and enhances 4E-BP1 expression.** In the current study, we used a transgenic mouse model that expresses a bicistronic mRNA containing two open reading frames (ORFs) encoding two distinct luciferase enzymes: LucR and LucF. Translation of the first ORF (LucR) occurs in a cap-dependent manner, whereas translation of the second ORF (LucF) is driven by the FGF-2 IRES that is located between the two cistrons (Fig. 1A). Similar transgenic mice have been used to demonstrate that diabetes leads to upregulated expression of FGF-2 by increased utilization of the FGF-2 IRES in the aorta (30). Four weeks after the induction of diabetes, blood glucose levels were raised from 189  $\pm$  12 to 540  $\pm$  26 mg/dL and the activity of the LucR reporter was reduced by 62% in the liver of mice with STZ-induced type 1 diabetes compared with nondiabetic littermates (Fig. 1B), whereas LucF activity was elevated by 192% (Fig. 1C). As a result, the relative LucF-to-LucR activity ratio was enhanced by 633% (Fig. 1D). To investigate a potential mechanism for mediating the shift from cap-dependent to cap-independent translation in the liver of STZ-treated mice, the interaction of 4E-BP1 and eIF4G with eIF4E was evaluated. The amount of 4E-BP1 bound to eIF4E was elevated in the liver of diabetic compared with control mice (Fig. 1E), whereas the amount of eIF4G bound to eIF4E was reduced (Fig. 1F). These changes were accompanied by decreased 4E-BP1 phosphorylation (Fig. 1G) and increased *O*-GlcNAcylation (Fig. 1H). Whereas the expression of eIF4E in the liver of STZ-treated and control mice was not different (Fig. 1I), total hepatic 4E-BP1 expression was increased (Fig. 1J) and likely contributed to increased interaction with eIF4E.

**Role of hyperglycemia in promoting cap-independent translation.** The role of hyperglycemia in mediating the diabetes-induced shift toward cap-independent translation was assessed using phlorizin treatment, which rapidly lowers blood glucose concentrations by blocking intestinal glucose absorption and producing renal glucosuria (31). Phlorizin treatment reduced the nonfasting blood glucose of mice with STZ-induced diabetes from a concentration of 539  $\pm$  22 to 300  $\pm$  16 mg/dL (Fig. 2A). LucR activity was repressed in the liver of diabetic compared with control mice, and upon phlorizin treatment its activity was elevated by 47% (Fig. 2A). Whereas LucF activity was elevated by 99% in diabetic compared with control mice, after treatment with phlorizin LucF activity was elevated by only 42% (Fig. 2C). Lowering blood glucose levels reduced the relative LucF-to-LucR ratio observed in the liver of diabetic mice by 52% (Fig. 2D). Phlorizin treatment of diabetic mice also reduced the amount of 4E-BP1 in eIF4E immunoprecipitates (Fig. 2E) and concomitantly elevated the interaction of eIF4E with eIF4G (Fig. 2F). The reduced

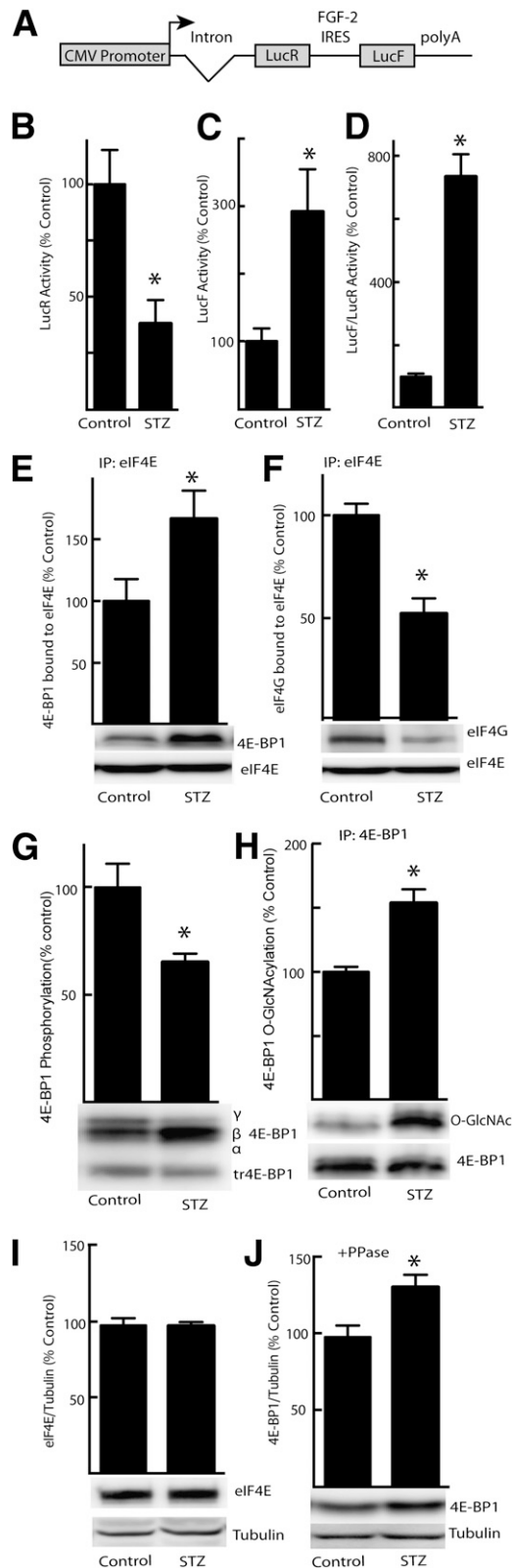


**FIG. 1.** STZ-induced diabetes produces a shift from cap-dependent to cap-independent translation. Liver supernatant fractions (1,000g) were prepared from transgenic mice after 4 weeks of STZ-induced diabetes or from control mice treated with vehicle only as described in RESEARCH DESIGN AND METHODS. **A:** Diagram of bicistronic transgene expressed by transgenic mice. **B:** Translation of LucR occurs in a cap-dependent manner. **C:** Translation of LucF is regulated by the FGF-2 IRES in a cap-independent manner. **D:** Ratio of LucF to LucR activity in liver supernatant fraction represents the relative translation from each reporter. The interaction of 4E-BP1 (**E**) and eIF4G (**F**) with eIF4E was

interaction of 4E-BP1 with eIF4E upon phlorizin treatment was likely in part due to lower 4E-BP1 expression (Fig. 2G) as well as increased phosphorylation (Fig. 2H) and decreased O-GlcNAcylation (Fig. 2I) of 4E-BP1 compared with untreated diabetic mice. Similar to previous findings with  $Ins2^{Akita/+}$  diabetic mice (11), phlorizin treatment attenuated the elevated hepatic expression of glutamine-fructose-6-phosphate amidotransferase (GFAT) (Fig. 2J) but did not alter total eIF4E expression (Fig. 2K).

**Hyperglycemia promotes cap-independent translation by increasing flux through the HBP.** GFAT is the rate-limiting enzyme of the HBP and as such regulates the production of UDP *N*-Acetylglucosamine, which serves as the substrate for protein O-GlcNAcylation. Changes in GFAT expression suggest that flux through the HBP plays an important role in mediating the effects of hyperglycemia on 4E-BP1 O-GlcNAcylation and expression. For further evaluation of the role of hyperglycemia and the HBP in cap-dependent and cap-independent translation, hepatocytes isolated from the liver of the transgenic bicistronic reporter mice were incubated in medium containing either 11 or 33 mmol/L glucose to match blood glucose concentrations observed in control and STZ-treated mice. Hyperglycemic conditions dramatically enhanced the relative cap-independent translation (Fig. 3A) and 4E-BP1 expression (Fig. 3B) without altering eIF4E expression (Fig. 3C). Immunoprecipitation of eIF4E revealed elevated interaction of 4E-BP1 with eIF4E in hepatocytes maintained in the presence of high compared with low glucose (Fig. 3D). When hepatocytes maintained in low glucose medium were treated with glucosamine to directly stimulate the HBP or thiamet G, a potent and selective inhibitor of O-GlcNAcase that dramatically elevates protein O-GlcNAcylation (32) by bypassing GFAT, total protein O-GlcNAcylation was enhanced (Fig. 3E). Similarly, both glucosamine and thiamet G enhanced the LucF-to-LucR activity ratio in hepatocytes when maintained in low glucose medium (Fig. 3F). Both glucosamine and thiamet G enhanced expression of 4E-BP1 (Fig. 3G) but not eIF4E (Fig. 3H), and immunoprecipitation of eIF4E revealed elevated interaction of 4E-BP1 with eIF4E (Fig. 3I). Overall, these findings support the conclusion that the hyperglycemia-induced shift from cap-dependent to cap-independent translation in protein O-GlcNAcylation that coincide with alterations in the expression of 4E-BP1 and its interaction with eIF4E.

**Ablation of 4E-BP1/2 prevents hyperglycemia-mediated shift from cap-dependent to cap-independent translation.** The role of hyperglycemia in modulating the shift from cap-dependent to cap-independent translation was further assessed using MEFs transiently transfected with bicistronic luciferase constructs in which the activity of LucR occurs in a cap-dependent manner and the activity of LucF is regulated by either the FGF-2 or the VEGF. Under high-compared with low-glucose conditions, the ratio of LucF

examined by immunoprecipitating eIF4E and measuring the amount of 4E-BP1 and eIF4G in the immunoprecipitate (IP) by Western blot analysis. Phosphorylation (**G**) and O-GlcNAcylation (**H**) of 4E-BP1 as well as total eIF4E (**I**) and 4E-BP1 (**J**) content was measured by treating supernatant fractions with  $\lambda$ -phosphatase (PPase) followed by Western blot analysis as previously described (11). Values are means  $\pm$  SE for a single experiment ( $n = 8$ ). Statistical significance of the differences between means was assessed by Student *t* test and is denoted by \* $P < 0.05$ .

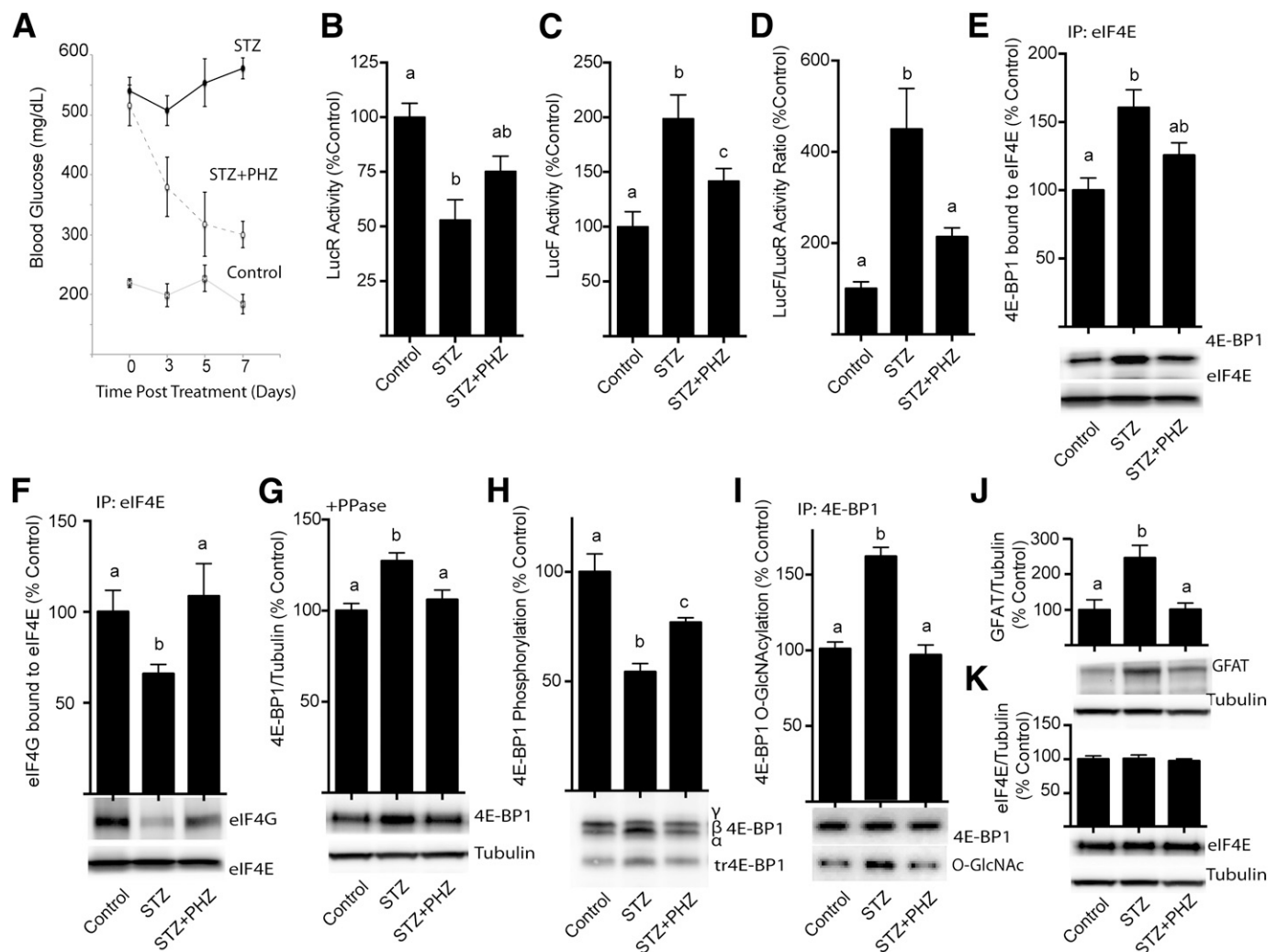


**FIG. 2.** Phlorizin lowers blood glucose concentrations in STZ-treated mice and represses the diabetes-induced shift from cap-dependent to cap-independent translation in liver. Diabetes was induced in transgenic mice by STZ injection. Four weeks after the induction of diabetes, control and STZ mice were subcutaneously injected with solvent or phlorizin (PHZ) twice daily for 7 days to lower blood glucose concentrations (A). B and C: Luciferase activity was assessed in 1,000g supernatant fractions from liver extracts. Translation of LucR is under control of the cytomegalovirus (CMV) promoter in a cap-dependent manner, and LucF is regulated by the FGF-2 IRES. D: Ratio of LucF to LucR activity in liver supernatant fraction. The interaction of 4E-BP1 (E) and eIF4G (F) with eIF4E was examined by immunoprecipitating eIF4E and measuring the amount of each protein in the immunoprecipitate (IP) by Western blot analysis. G: 4E-BP1 content was measured by treating the supernatant fraction with  $\lambda$ -phosphatase (PPase) followed by Western blot analysis as previously described (11). H: Phosphorylation of 4E-BP1 was assessed as the ratio of the protein in the hyperphosphorylated  $\gamma$ -isoform to the total amount of 4E-BP1 in all isoforms. I: O-GlcNAcylation of 4E-BP1 was assessed by immunoprecipitating 4E-BP1 and measuring the amount of O-GlcNAcylation (O-GlcNAc) by Western blot relative to the total amount of 4E-BP1. Total content of GFAT (J) and eIF4E (K) was assessed by Western blot analysis. Values are means  $\pm$  SE for two independent experiments ( $n = 8$ ). Statistical significance was assessed by ANOVA followed by Holm-Sidak multiple-comparisons test to compare the mean of each group with the mean of every other group. Statistical significance is denoted by the presence of different letters above the bars on the graphs. Bars with different letters are statistically different;  $P < 0.05$ .

to LucR activity increased by 20% for the FGF-2 IRES and 77% for the VEGF IRES (Fig. 4A). Further, the ratio of LucF to LucR activity with the VEGF IRES also increased by 79% when cells maintained in low-glucose medium were treated with glucosamine (Fig. 4B). When wild-type and 4E-BP1/2 knockout (*Eif4ebp1;Eif4ebp2*) MEFs were analyzed after transient transfection with the bicistronic luciferase constructs containing the VEGF IRES, the expression of 4E-BP1 was increased by 72% in cells maintained in medium containing high glucose and treated with glucosamine compared with the low-glucose condition (Fig. 4C). There was no detectable 4E-BP1 under either condition in knockout cells. Exposure to high glucose and glucosamine increased the ratio of LucF to LucR activity in wild-type cells to 333% that of the low-glucose condition. In contrast, there was no

effect on the ratio of LucF to LucR activity with treatment of 4E-BP1/2 knockout cells (Fig. 4D). For confirmation of the role of 4E-BP1 specifically, hepatocytes from 4E-BP1/2 knockout mice were transfected with a bicistronic plasmid containing the IRES for VEGF and maintained in medium containing either low glucose or high glucose with glucosamine. There was no significant difference in the ratio of LucF to LucR activity under the high- and low-glucose conditions for 4E-BP1 knockout hepatocytes, whereas high glucose increased the ratio of LucF to LucR activity in 4E-BP2 knockout hepatocytes to 234% that of the low-glucose condition (Fig. 4E). These results demonstrate that expression of 4E-BP1 but not 4E-BP2 is necessary for the hyperglycemia-induced shift from cap-dependent to cap-independent translation.

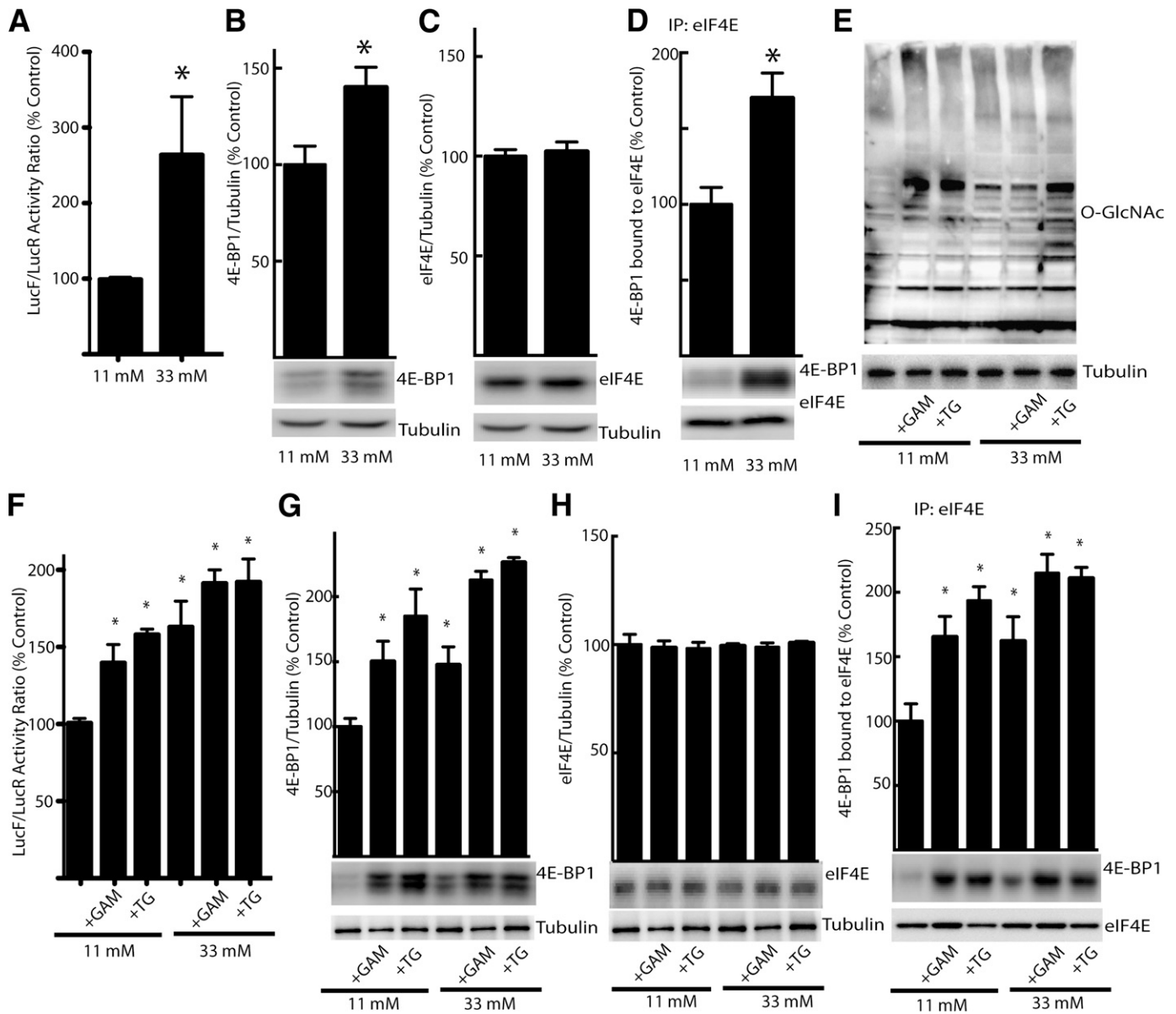


**FIG. 3.** Hyperglycemic conditions mediate a shift in translation of FGF-2 reporter from cap-dependent to cap-independent translation in isolated hepatocytes and enhance 4E-BP1 expression via the HBP. For evaluation of the role of the HBP, hepatocytes isolated from transgenic mice were maintained in medium containing 11 or 33 mmol/L glucose for 24 h followed by exposure to 3 mmol/L glucosamine (GAM), which feeds directly into the pathway, or thiamet G (TG), an inhibitor of *O*-GlcNAcase. **A** and **F**: The relative translation of LucR and LucF was evaluated. The expression of 4E-BP1 (**B** and **G**) as well as eIF4E (**C** and **H**) was assessed in 1,000g cell supernatant fractions by Western blot analysis. **D** and **I**: The interaction of 4E-BP1 with eIF4E was examined by immunoprecipitating eIF4E and measuring the amount of 4E-BP1 in the immunoprecipitate (**IP**) by Western blot analysis. **E**: Total protein *O*-GlcNAcylation (*O*-GlcNAc) was assessed in cell supernatant fractions by Western blot. Values are means + SE for two independent experiments ( $n = 4$ ). Statistical significance of the differences between means was assessed by Student *t* test and is denoted by \* $P < 0.05$ .

**pSILAC identifies proteins with altered synthetic rates under hyperglycemic conditions.** To identify hyperglycemia-induced changes in the translational control of protein expression on a global scale, we used pSILAC to evaluate newly synthesized proteins and quantitate changes in their accumulation rates in MEFs in the presence of either low glucose or high glucose supplemented with glucosamine, as these conditions produced the largest increase in the LucF-to-LucR ratio (Fig. 4B). In total, 1,355 and 2,905 proteins were identified with high confidence in two independent runs. While the majority of proteins had medium-to-heavy ratios of ~1:1, indicating that their translation was not significantly altered by

hyperglycemic conditions, the synthesis of a number of proteins was significantly altered between the two conditions. The top-scoring proteins whose synthesis was either upregulated or repressed under high- compared with low-glucose condition are listed in Tables 1 and 2, respectively.

In the classic model of cap-dependent translation initiation, ribosome scanning of the 5'-UTR is impaired by strong secondary structures. Characteristics that decrease the efficiency of cap-dependent translation include the length of the 5'-UTR and the complexity of secondary structure (33). Thus, we predicted that the high-glucose condition would repress the translation of mRNAs with

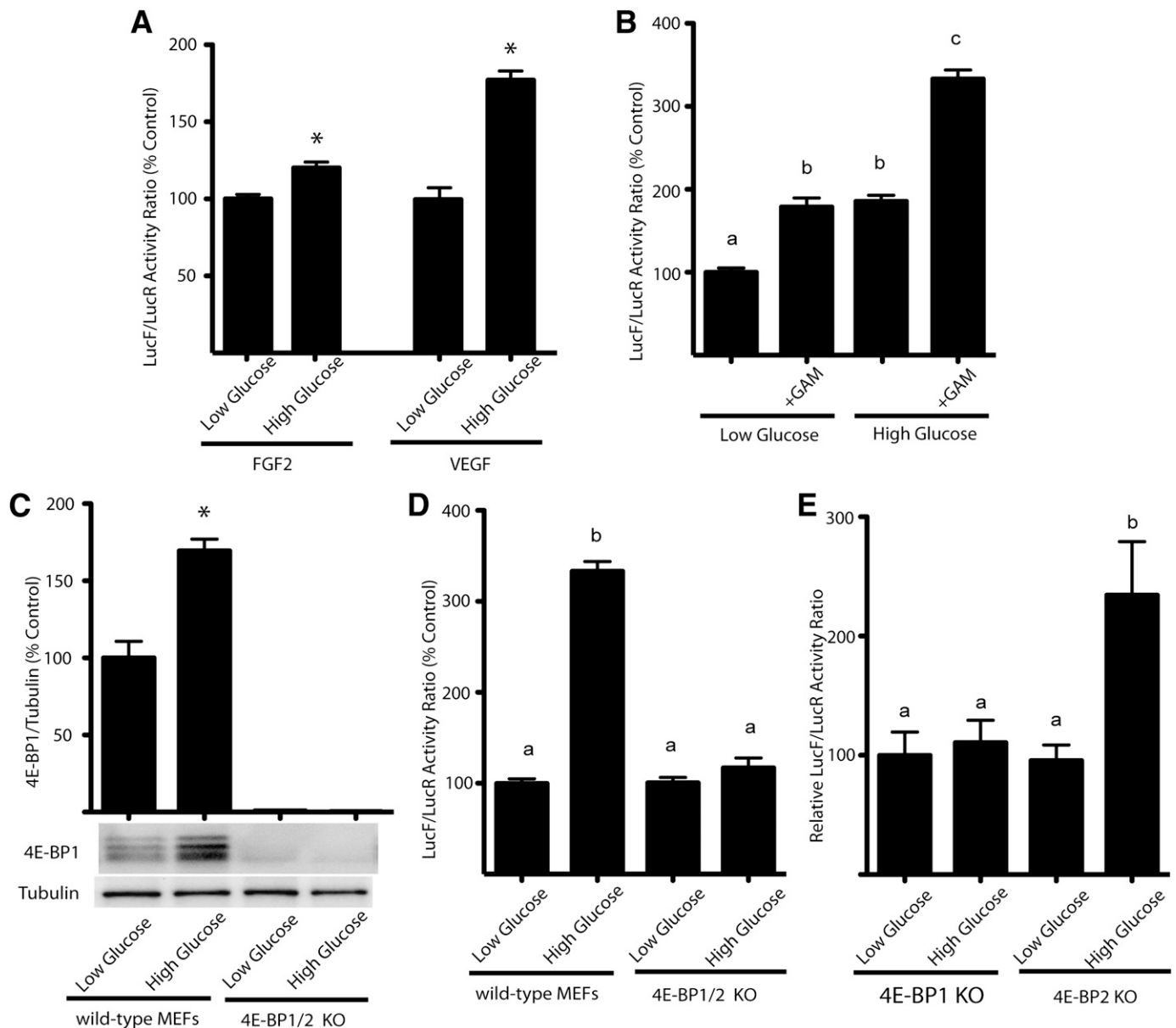


**FIG. 4.** Hyperglycemic conditions mediate a shift from cap-dependent to cap-independent translation that is dependent on 4E-BP1. **A:** MEFs were incubated in medium containing high (25 mmol/L glucose) or low (5 mmol/L glucose, 20 mmol/L mannitol) glucose. Cells were transiently transfected with a bicistronic plasmid containing the IRES for either FGF-2 or VEGF. Whole-cell lysates were harvested, and the relative translation of LucR and LucF was evaluated. **B:** MEF cells were transiently transfected with bicistronic luciferase plasmid containing the VEGF IRES and were incubated in either 5 or 25 mmol/L glucose in the presence and absence of 3 mmol/L glucosamine. **C:** Wild-type and *Eif4ebp1;Eif4ebp2* double knockout MEFs were incubated in medium containing either low glucose or high glucose with 3 mmol/L glucosamine. The content of 4E-BP1 relative to tubulin was assessed in whole-cell lysates by Western blot analysis. **D:** Whole-cell lysates were prepared, and the relative translation of LucR and LucF was evaluated. Values are means  $\pm$  SE for two independent experiments ( $n = 4$ ). **E:** Hepatocytes from *Eif4ebp1;Eif4ebp2* knockout mice were transfected with a bicistronic plasmid containing the IRES for VEGF and maintained in medium containing either low glucose or high glucose with 3 mmol/L glucosamine. Values are means  $\pm$  SE for two independent experiments ( $n = 3$ ). Statistical significance was assessed by either Student *t* test or ANOVA followed by Holm-Sidak multiple-comparisons test to compare the mean of each group with the mean of every other group. Statistical significance is denoted by \* (A and C) or the presence of different letters above the bars on the graphs (B, D, and E). Bars with different letters are statistically different;  $P < 0.05$ .

less complex 5'-UTRs in favor of mRNAs with more structured 5'-UTRs. Most cellular IRES elements are 150–300 nucleotides in length, although some are as short as 22 nucleotides (34). The mRNA-encoding proteins whose synthesis was upregulated by high glucose averaged 185.3 nucleotides in length and were 74% longer than the average number of nucleotides in 5'-UTRs of mRNAs encoding proteins whose synthesis was downregulated by high glucose (Fig. 5A). To investigate the complexity of these 5'-UTRs, we used mfold (<http://mfold.rna.albany.edu/>?

$q=$ mfold) to compute secondary structures and calculate a corresponding free energy change for folding ( $\Delta G$ ). The top-scoring proteins whose synthesis was downregulated by high-glucose conditions have an average  $\Delta G$  of  $-41.1$  kcal/mol, whereas the top-scoring proteins whose synthesis was upregulated by high-glucose conditions have a significantly lower average  $\Delta G$  value of  $-77.5$  kcal/mol, indicative of more stable secondary structures (Fig. 5B). To verify that the hyperglycemia-induced enhancement in the synthetic rates of proteins with longer 5'-UTRs was not

TABLE 1  
Top proteins identified by pSILAC with elevated synthetic rates in cells exposed to hyperglycemic conditions

Accession no.	RefSeq ID	Name	%Cov (95)	Peptides (95%)	M:H	P
8393135	NM_016904	Cyclin-dependent kinases regulatory subunit 1	32.91	2	0.01	0.017
27734154	NM_173413	ras-related protein Rab-8B	27.05	5	0.01	0.015
6756037	NM_011738	14-3-3 protein $\eta$	24.80	6	0.01	0.000
31542228	NM_007544	BH3-interacting domain death agonist	18.46	2	0.01	0.014
6755100	NM_011119	Proliferation-associated protein 2G4	17.77	5	0.01	0.016
110625776	NM_027412	Tetratricopeptide repeat protein 9C	16.96	2	0.01	0.014
21313588	NM_024499	Small glutamine-rich tetratricopeptide repeat-containing protein $\alpha$	15.56	4	0.01	0.018
6755478	NM_011358	Serine/arginine-rich splicing factor 2	14.93	3	0.01	0.014
47059484	NM_009030	Histone-binding protein RBBP4	14.59	7	0.01	0.014
6754450	NM_010634	Fatty acid-binding protein, epidermal	14.07	2	0.01	0.014
169790909	NM_023514	28S ribosomal protein S9, mitochondrial precursor	13.33	4	0.01	0.015
295789090	NM_001177965	<i>N</i> - $\alpha$ -acetyltransferase 10 isoform 2	13.33	2	0.01	0.014
32441290	NM_027133	Protein lunapark isoform a	12.94	3	0.01	0.015
6678145	NM_009279	Translocon-associated protein subunit $\Delta$ isoform 2 precursor	12.79	3	0.01	0.014
117647257	NM_023554	Nucleolar protein 7	11.02	2	0.01	0.014
31560168	NM_026487	ATPase family AAA domain-containing protein 1	10.53	2	0.01	0.014
9789907	NM_019719	STIP1 homology and U box-containing protein 1	10.53	3	0.01	0.013
21313618	NM_025336	Coiled-coil-helix-coiled-coil-helix domain-containing protein 3	8.81	2	0.01	0.014
258679524	NM_001164838	Leucine-rich repeat flightless-interacting protein 2 isoform 1	7.95	2	0.01	0.014
6671549	NM_007453	Peroxiredoxin-6	7.59	1	0.01	0.017
160707921	NM_013469	Annexin A11	7.16	3	0.01	0.014
30409972	NM_178398	WD repeat domain phosphoinositide-interacting protein 2	6.52	2	0.01	0.014
198278501	NM_027879	Pre-mRNA-processing factor 17	5.70	2	0.01	0.014
31980960	NM_019586	Ubiquitin-conjugating enzyme E2 J1	5.35	1	0.01	0.014
6755382	NM_011304	ruvB-like 2	5.18	2	0.01	0.000
311893360	NM_001198867	Dynactin subunit 1 isoform 3	4.12	4	0.01	0.013
22122591	NM_146093	UBX domain-containing protein 1	4.04	1	0.01	0.016
255683374	NM_145610	Suppressor of SWI4 1 homolog	3.83	1	0.01	0.014
356995938	NM_001252442	Pleckstrin homology-like domain family B member 2	3.46	4	0.01	0.013
87299619	NM_001039522	RNA polymerase-associated protein LEO1	3.45	2	0.01	0.014
6753550	NM_012006	Acyl-CoA thioesterase 1	3.34	1	0.01	0.015
6679553	NM_008977	Tyrosine protein phosphatase nonreceptor	2.88	1	0.01	0.014
6755674	NM_011490	Double-stranded RNA-binding protein Staufen	2.67	1	0.01	0.014
268838020	NM_026423	Methylthioribose-1-phosphate isomerase	2.44	2	0.01	0.013
28892935	NM_177045	Coiled-coil and C2 domain-containing protein 1B	2.01	1	0.01	0.014
21312638	NM_028015	Ceramide synthase 5	1.93	1	0.01	0.014
267844920	NM_021714	WW domain-binding protein 11	1.87	1	0.01	0.013
68299824	NM_181072	Myosin IE	1.81	2	0.01	0.014
255982530	NM_001164223	Replication protein A 70-kDa DNA-binding subunit	1.71	1	0.01	0.000
52138536	NM_178930	Golgi-specific brefeldin A-resistance GEF 1	1.61	2	0.01	0.013
341604762	NM_001045513	Ras association (RalGDS/AF-6) and pleckstrin homology domains 1 iso 3	1.11	1	0.01	0.014
120300971	NM_053204	ELKS/Rab6-interacting/CAST family member 1 isoform 1	1.07	1	0.01	0.014
258547119	NM_001164662	Cytoplasmic FMR1-interacting protein 1 isoform b	1.04	1	0.01	0.000
146231996	NM_021523	E3 ubiquitin-protein ligase HUWE1	0.53	2	0.01	0.014
30519943	NM_178614	Sorting and assembly machinery component 50 homolog	0.00	0	0.01	0.013

Cultures of wild-type MEFs were maintained in Dulbecco's modified Eagle's medium containing either 5 or 25 mmol/L glucose. For the low-glucose condition, cells were then labeled for 6 h by pSILAC using 5 mmol/L glucose supplemented with 20 mmol/L mannitol and labeled with 4,4,5,5-D<sub>4</sub>-L-lysine monohydrochloride and L-arginine-<sup>13</sup>C<sub>6</sub>. For the high-glucose condition, MEF cultures were maintained in 25 mmol/L glucose supplemented with 3 mmol/L glucosamine and labeled with media containing L-lysine-<sup>13</sup>C<sub>6</sub> <sup>15</sup>N<sub>2</sub> monohydrochloride and L-arginine-<sup>13</sup>C<sub>6</sub> <sup>15</sup>N<sub>4</sub> monohydrochloride. Cells were harvested, combined, and analyzed by mass spectrometry to compare labeled peptide peaks. Statistical significance was assessed by Student *t* test on the average of all ratio values for the peptides associated with each particular protein. %Cov (95), the percentage of matching amino acids from identified peptides having confidence greater than or equal to 95 divided by the total number of amino acids in the sequence.

TABLE 2  
Top proteins identified by pSILAC with repressed synthetic rates in cells exposed to hyperglycemic conditions

Accession no.	RefSeq ID	Name	%Cov (95)	Peptides (95%)	M:H	<i>P</i>
71480098	NM_001024622	PEST proteolytic signal-containing nuclear protein	27.53	3	100	0.016
18702317	NM_016900	Caveolin-2	22.22	2	100	0.015
21426823	NM_030609	Histone H1.1	20.19	6	100	0.015
13384730	NM_025364	SAP domain-containing ribonucleoprotein	20.00	3	100	0.000
6677691	NM_009037	Reticulocalbin-1 precursor	13.85	5	100	0.000
19705424	NM_009439	26S proteasome non-ATPase regulatory subunit 3	13.02	3	100	0.014
6753412	NM_011801	Craniofacial development protein 1	12.88	3	100	0.014
170932536	NM_007916	ATP-dependent RNA helicase DDX19A	12.55	6	100	0.015
160707909	NM_009499	Vasodilator-stimulated phosphoprotein	11.20	3	100	0.015
152963551	NM_177374	tRNA [adenine(58)-N(1)]-methyltransferase catalytic subunit TRMT61A	10.69	2	100	0.015
339895909	NM_001243041	Adenosine kinase isoform 2	7.25	2	100	0.014
13385590	NM_026091	UPF0687 protein C20orf27 homolog	6.90	1	100	0.013
19072792	NM_029572	Endoplasmic reticulum resident protein 44 precursor	6.90	2	100	0.016
239735501	NM_027008	BTB/POZ domain-containing protein KCTD5	6.84	1	14	0.083
21704100	NM_145558	Trifunctional enzyme subunit $\beta$ , mitochondrial precursor	6.11	2	100	0.015
13385878	NM_026386	Sorting nexin-2	5.78	2	100	0.014
6753364	NM_009861	Cell division control protein 42 homolog isoform 1 precursor	5.76	3	100	0.019
124358934	NM_001024526	la-related protein 4 isoform 1	5.29	2	100	0.017
268836255	NM_133198	Glycogen phosphorylase, liver form	4.82	3	100	0.013
70780373	NM_017476	A-kinase anchor protein 8-like	4.52	2	100	0.013
21704176	NM_145585	THUMP domain-containing protein 1	4.29	1	85	0.002
6755847	NM_011622	Target of Myb protein 1 isoform 1	4.06	1	100	0.016
270309140	NM_133780	Nuclear pore complex-associated protein Tpr	3.83	8	15	0.096
31541932	NM_144874	Cytochrome c oxidase assembly protein COX15 homolog	3.39	1	74	0.047
307938353	NM_133885	Oxysterol-binding protein-related protein 9 isoform a	3.04	2	100	0.014
25188204	NM_027869	Polyribonucleotide nucleotidyltransferase 1, mitochondrial precursor	2.94	2	100	0.015
226442882	NM_001033528	Ubiquitin carboxyl-terminal hydrolase 36	2.91	2	100	0.014
145587092	NM_010806	Afadin	2.86	3	100	0.016
161702988	NM_009693	Apolipoprotein B precursor	2.75	15	50	0.018
23943807	NM_153507	Copine-2	2.74	1	100	0.015
188219597	NM_011258	Replication factor C subunit 1	2.56	3	100	0.014
66955886	NM_175310	Sister chromatid cohesion protein PDS5 homolog B	2.35	2	100	0.015
162951865	NM_009594	Tyrosine-protein kinase ABL1 isoform b	2.32	2	100	0.014
229608895	NM_133815	Lamin-B receptor	2.24	1	100	0.014
78000177	NM_001034963	Sorbin and SH3 domain-containing protein 1 isoform 4	1.66	1	100	0.014
356995938	NM_001252442	Pleckstrin homology-like domain family B member 2 isoform 1	1.46	1	36	0.037
124487057	NM_001081213	Endoplasmic reticulum metalloproteinase 1	1.22	1	100	0.013

Cultures of wild-type MEFs were maintained in Dulbecco's modified Eagle's medium containing either 5 or 25 mmol/L glucose. For the low-glucose condition, cells were then labeled for 6 h by pSILAC using 5 mmol/L glucose supplemented with 20 mmol/L mannitol and labeled with 4,4,5,5-D<sub>4</sub>-L-lysine monohydrochloride and L-arginine-<sup>13</sup>C<sub>6</sub>. For the high-glucose condition, MEF cultures were maintained in 25 mmol/L glucose supplemented with 3 mmol/L glucosamine and labeled with media containing L-lysine-<sup>13</sup>C<sub>6</sub>, <sup>15</sup>N<sub>2</sub> monohydrochloride and L-arginine-<sup>13</sup>C<sub>6</sub>, <sup>15</sup>N<sub>4</sub> monohydrochloride. Cells were harvested, combined, and analyzed by mass spectrometry to compare labeled peptide peaks. Statistical significance was assessed by Student *t* test on the average of all ratio values for the peptides associated with each particular protein. %Cov (95), the percentage of matching amino acids from identified peptides having confidence greater than or equal to 95 divided by the total number of amino acids in the sequence.

the result of elevated mRNA transcription, we evaluated the abundance of mRNAs corresponding to six proteins from Table 1 with the longest 5'-UTRs (Fig. 5C). Of the six analyzed, only one exhibited increased abundance, and that was 50-fold less than the accumulation of newly synthesized protein. Changes in protein degradation may also impact the M-to-H ratio observed during pSILAC; however, its contribution is relatively small (35). These findings suggest that hyperglycemia favors the translation of messages with longer/more highly structured 5'-UTRs. Although

no proteins encoded by mRNAs containing known IRES structures were identified among the top-scoring upregulated proteins, several proteins were identified whose mRNAs are listed on IRESite, the database of experimentally verified IRES structures (36). Among these, cellular inhibitor of apoptosis 1 (c-IAP1) (gil133922596), heat shock 70-kDa protein 1A (HSPA1A) (gil40254361), cold shock domain containing E1 (UNR) (gil240255574), and utrophin A (UTRA) (gil110431378) were all elevated by nearly twofold in cells exposed to high-glucose conditions

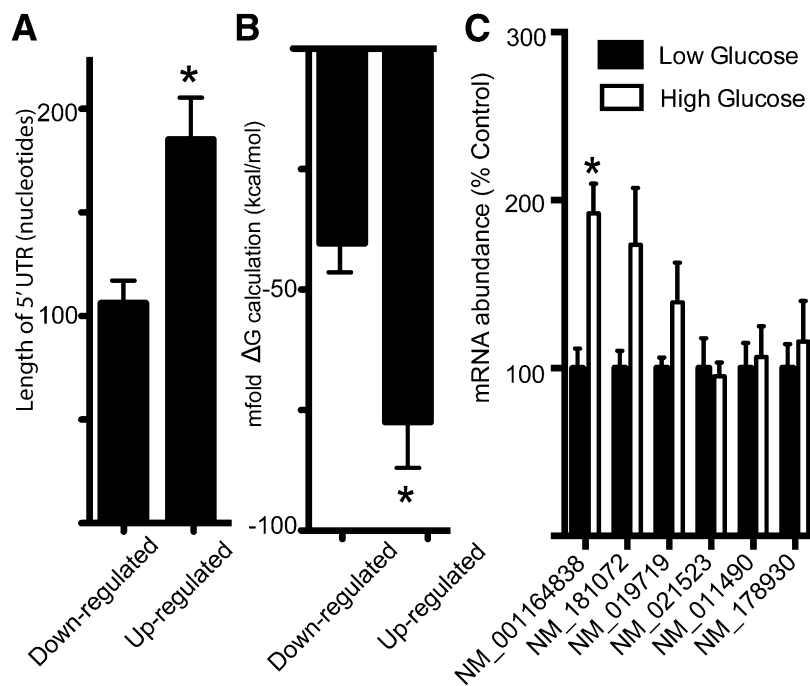


**FIG. 5.** Hyperglycemic conditions upregulate translation of mRNAs with more complex 5'-UTRs. The database of transcriptional start sites (dbTSS [http://dbtss.hgc.jp/]) was used to identify the 5'-UTRs of the top-scoring proteins identified by pSILAC with altered expression after incubation of MEFs in medium containing either 5 mmol/L glucose supplemented with 20 mmol/L mannitol or with 25 mmol/L glucose supplemented with 3 mmol/L glucosamine. The list of these proteins can be found in Tables 1 and 2. *A*: The average 5'-UTR length for the mRNAs of the top-scoring proteins was calculated. *B*: Secondary structures of 5'-UTRs for the mRNAs of the top-scoring proteins were computed with mfold (http://mfold.rna.albany.edu/?q=mfold) to generate a corresponding free energy change for folding ( $\Delta G$ ). For reference, Kozak (45) found that 5' sequences with predicted  $\Delta G$  values of  $-30$  kcal/mol had no effect on translation, whereas those with predicted  $\Delta G$  values of  $-50$  kcal/mol reduced cap-dependent translation by 85–95%, suggesting that the 43S PIC can melt moderately stable structures but stalls at more stable structures. *C*: RNA was extracted from MEF whole-cell lysates after a standard TRIzol protocol. mRNA expression was normalized to internal controls for glyceraldehyde-3-phosphate dehydrogenase and  $\alpha$ -tubulin. All values are means  $\pm$  SE for two independent experiments ( $n = 37$ – $45$  for *A* and *B*;  $n = 6$  for *C*). Statistical significance of the differences between means was assessed by Student *t* test and is denoted as \* $P < 0.05$ .

in two independent runs, while BCL2 (gil6753200) increased by nearly 80-fold in the second run but was not detected in the initial run.

Functional relationships between genes that were differentially expressed in low and high glucose were investigated with IPA. IPA showed that the proteins whose accumulation was upregulated are associated with pathways that regulate eIF2, eIF4F, and S6K1 signaling; protein ubiquitination; and aminoacyl-tRNA biosynthesis (Table 3). Further, the most significant toxicologic list pathways were hypoxia-inducible factor (HIF) signaling, oxidative stress mediated by nuclear factor erythroid 2-related factor 2 (Nrf2), mitochondrial dysfunction, and DNA damage checkpoint regulation of cell cycle phase G2/M (Table 3). Both HIF-1 and Nrf2 contain IRES sequences in their 5'-UTR that allow their translation to be maintained under stress conditions that are inhibitory to cap-dependent translation (6,37). IPA was also used to predict which mRNAs encoding transcription factors were most likely responsible for the altered pattern of expression under low- and high-glucose conditions. The top transcription factor altered by high glucose was the proto-oncogene *myc* (Table 3), whose 5'-UTR contains an IRES. Activation of *myc* was predicted under high-glucose conditions based on a broad network of interacting proteins (Supplementary Fig. 1).

## DISCUSSION

The findings of the current study provide insight into a novel mechanism through which diabetes-induced

hyperglycemia alters the selection of mRNA for translation. In the liver of diabetic mice, 4E-BP1 exhibited reduced phosphorylation, elevated O-GlcNAcylation, and enhanced interaction with eIF4E compared with nondiabetic mice. These alterations in 4E-BP1 were associated with a shift from cap-dependent to cap-independent translation using bicistronic luciferase reporter assays. For demonstration of the component of the diabetic state responsible for this shift, diabetic mice were treated with phlorizin to reduce blood glucose concentrations. When the blood glucose concentration was lowered, the interaction of 4E-BP1 with eIF4E returned to nondiabetic levels and the shift from cap-dependent to cap-independent reporter activity was reversed. A similar shift toward cap-independent mRNA translation was observed with cells in culture upon exposure to hyperglycemic conditions or under conditions that promoted protein O-GlcNAcylation. O-GlcNAcylation of 4E-BP1 correlated with the hyperglycemia-induced shift from cap-dependent to cap-independent translation, and expression of 4E-BP1 was necessary for this effect. We extended these findings using pSILAC to identify novel proteins that undergo altered rates of synthesis in high- versus low-glucose conditions. Examination of the expression pattern of these proteins revealed a hyperglycemia-induced shift toward proteins with more complex 5'-UTRs. Overall, the results are consistent with a model wherein the O-GlcNAcylation of 4E-BP1 results in elevated expression and promotes its interaction with eIF4E (11), thereby altering gene expression in response to hyperglycemia and diabetes.

TABLE 3  
IPA of protein synthetic rates in cells exposed to hyperglycemic conditions

	<i>P</i>	Ratio
Top canonical pathways		
EIF2 signaling	3.66E-28	67:205
Protein ubiquitination pathway	1.79E-20	68:269
Regulation of eIF4 and p70S6 K signaling	1.55E-18	48:176
Aminoacyl-tRNA biosynthesis	3.21E-11	17:76
Top toxicologic lists		
HIF signaling	3.40E-06	18:70
NRF2-mediated oxidative stress response	2.04E-04	34:234
Mitochondrial dysfunction	2.96E-08	23:138
Cell cycle: G2/M DNA damage checkpoint regulation	9.45E-03	9:48
Top transcription factors		
MYC	9.02E-40	
MYCN	1.39E-22	
NFE2L2	6.37E-14	
XBP1 (includes EG: 140614)	4.28E-10	
HSF2	3.27E-07	

Cultures of wild-type MEF were maintained in Dulbecco's modified Eagle's medium containing either 5 or 25 mmol/L glucose. For the low-glucose condition, cells were then labeled for 6 h by pSILAC using 5 mmol/L glucose supplemented with 20 mmol/L mannitol and labeled with 4,4,5,5-D<sub>4</sub>-L-lysine monohydrochloride and L-arginine-<sup>13</sup>C<sub>6</sub>. For the high-glucose condition, MEF cultures were maintained in 25 mmol/L glucose supplemented with 3 mmol/L glucosamine and labeled with L-lysine-<sup>13</sup>C<sub>6</sub> <sup>15</sup>N<sub>2</sub> monohydrochloride and L-arginine-<sup>13</sup>C<sub>6</sub> <sup>15</sup>N<sub>4</sub> monohydrochloride. Cells were harvested, combined, and analyzed by mass spectrometry to compare labeled peptide peaks. The raw data obtained from pSILAC analysis were uploaded and analyzed using proteome software IPA (www.ingenuity.com) to identify functionally grouped gene sets and pathways that were upregulated under hyperglycemic conditions.

Regulation of the initiation complex eIF4F by post-translational modification is of critical importance in the selection of mRNAs for cap-dependent translation initiation. Binding of hypophosphorylated 4E-BP1 to eIF4E, which is mutually exclusive of interaction with eIF4G, prevents assembly of functional eIF4F complexes to repress loading of ribosomes onto the mRNA 5'-cap. The interaction of 4E-BP1 with eIF4E is not only regulated by phosphorylation; *O*-GlcNAcylation of 4E-BP1 also enhances its binding to eIF4E independent of 4E-BP1 phosphorylation status (10). Thus, hyperglycemia-induced sequestration of eIF4E potentially downregulates the synthesis of a broad array of proteins. However, under conditions where eIF4E is limiting, the same canonical initiation factors can facilitate the cap-independent loading of ribosomes onto mRNA that contain IRES elements (8). Therefore, by reducing the competition from capped mRNAs, hyperglycemia-induced sequestration of eIF4E potentially acts as a positive regulator of cap-independent translation in response to conditions of stress.

A critical role for 4E-BP1 in upregulating cap-independent translation has previously been demonstrated (38). Viral IRES-mediated translation is promoted when cellular cap-dependent translation is diminished under conditions of cellular stress (38). However, 4E-BP1 knockdown prevents upregulation of viral cap-independent translation under conditions of amino acid starvation (39). Furthermore, 4E-BP1 plays a crucial role in mediating differential protein expression during hypoxia (40). Overexpressed 4E-BP1 and eIF4G mediate a hypoxia-activated switch from cap-dependent to cap-independent mRNA translation

that promotes increased tumor angiogenesis and growth (41). It has been previously demonstrated that the presence of 4E-BP1/2 is also necessary for increased expression of VEGF in both the retina during diabetes and cells maintained under hyperglycemic conditions (42). The results of the current study suggest that increased VEGF expression occurs through increased use of internal ribosome entry sites in response to increased flux through the HBP. This finding likely extends to other mRNAs that are translated through an IRES-dependent mechanism, as overexpression of *O*-GlcNAcylation transferase produces an accumulation of 80S monosomes, suggesting that excessive *O*-GlcNAcylation suppresses translation initiation (23).

To explore the effect of hyperglycemia on mRNA translation, we used pSILAC to identify proteins that undergo altered rates of synthesis. Hyperglycemia promoted translation of mRNAs that contained long and structured 5'-UTRs, a characteristic associated with mRNAs containing IRES. This observation does not directly indicate that hyperglycemic conditions favor translation of all mRNAs with IRES domains. Instead, it is more likely that hyperglycemia-induced modification of the translational machinery enhances translation of a specific subset of messages, some of which contain IRES domains. In this study, hyperglycemia specifically enhanced IRES-mediated translation from luciferase reporters driven by either the FGF-2 or VEGF IRES sequence. Using pSILAC, we also observed increased translation of the following cellular mRNAs that have been previously shown to contain IRES structures: B-cell lymphoma 2 (BCL2), 78-kDa glucose-regulated protein (BiP), c-IAP1, HSPA1A, Runt-related transcription factor 1 (RunX1), UNR, and UTRA. IRES containing mRNAs often encode proteins with crucial biological functions, such as the major vascular growth factors VEGF, FGF-2, platelet-derived growth factor, and RunX1. Thus, enhanced hyperglycemia-mediated translation of angiogenic proteins potentially disrupts the relative balance of inducers and inhibitors of angiogenesis to promote the neurovascular complications associated with diabetes. Furthermore, our data support a previous microarray analysis of the retinal transcriptome where normalization of systemic glycemia in diabetic rats primarily restored pathways associated with growth factor signaling (43).

A functional link between the metabolic abnormalities associated with disease and regulation of IRES sequences has previously been proposed (44), yet direct evidence remains limiting. In the current study, we find that hyperglycemia and conditions that promote protein *O*-GlcNAcylation enhance IRES-mediated mRNA translation through a mechanism that is dependent on 4E-BP1. Thus, regulation of 4E-BP1 expression by *O*-GlcNAcylation represents a novel mechanism for altering the selection of mRNAs for translation under pathophysiological conditions. Elucidation of molecular mechanisms underlying cap-independent translation initiation will not only enhance our understanding of gene expression but also impact the development of treatment strategies for addressing the pathophysiology of diabetes.

#### ACKNOWLEDGMENTS

The research reported here was supported by National Institutes of Health grants DK088416 (to M.D.D.) and DK13499 (to L.S.J.).

No potential conflicts of interest relevant to this article were reported.

M.D.D. researched data and wrote and edited the manuscript. J.S.S. contributed to discussion and reviewed the manuscript. B.A.S. researched data, wrote the manuscript, contributed to discussion, and reviewed and edited the manuscript. S.R.K. and L.S.J. designed experiments, contributed to discussion, and reviewed and edited the manuscript. M.D.D. is the guarantor of this work and as such had full access to all the data in the study and takes responsibility for the integrity of the data and the accuracy of the data analysis.

Parts of this study were presented in abstract form at the 72nd Scientific Sessions of the American Diabetes Association, Philadelphia, Pennsylvania, 8–12 June 2012.

The authors thank Dr. N. Sonenberg (McGill University) for kindly providing 4E-BP1/2 DKO MEFs and Dr. A.-C. Prats (INSERM) for providing the bicistronic reporter containing the FGF-2 IRES. The authors also thank W. Dunton (Pennsylvania State University College of Medicine) and M. Wu (Pennsylvania State University College of Medicine) for assistance with animals.

## REFERENCES

- Pestova TV, Kolupaeva VG, Lomakin IB, et al. Molecular mechanisms of translation initiation in eukaryotes. *Proc Natl Acad Sci USA* 2001;98:7029–7036
- López-Lastra M, Rivas A, Barriá MI. Protein synthesis in eukaryotes: the growing biological relevance of cap-independent translation initiation. *Biol Res* 2005;38:121–146
- Hellen CU, Sarnow P. Internal ribosome entry sites in eukaryotic mRNA molecules. *Genes Dev* 2001;15:1593–1612
- Holcik M, Sonenberg N, Korneluk RG. Internal ribosome initiation of translation and the control of cell death. *Trends Genet* 2000;16:469–473
- Stein I, Itin A, Einat P, Skaliter R, Grossman Z, Keshet E. Translation of vascular endothelial growth factor mRNA by internal ribosome entry: implications for translation under hypoxia. *Mol Cell Biol* 1998;18:3112–3119
- Lang KJ, Kappel A, Goodall GJ. Hypoxia-inducible factor-1 $\alpha$  mRNA contains an internal ribosome entry site that allows efficient translation during normoxia and hypoxia. *Mol Biol Cell* 2002;13:1792–1801
- Fernandez J, Yaman I, Mishra R, et al. Internal ribosome entry site-mediated translation of a mammalian mRNA is regulated by amino acid availability. *J Biol Chem* 2001;276:12285–12291
- Pestova TV, Hellen CU, Shatsky IN. Canonical eukaryotic initiation factors determine initiation of translation by internal ribosomal entry. *Mol Cell Biol* 1996;16:6859–6869
- Svitkin YV, Herdy B, Costa-Mattioli M, Gingras AC, Raught B, Sonenberg N. Eukaryotic translation initiation factor 4E availability controls the switch between cap-dependent and internal ribosomal entry site-mediated translation. *Mol Cell Biol* 2005;25:10556–10565
- Gingras AC, Kennedy SG, O’Leary MA, Sonenberg N, Hay N. 4E-BP1, a repressor of mRNA translation, is phosphorylated and inactivated by the Akt(PKB) signaling pathway. *Genes Dev* 1998;12:502–513
- Dennis MD, Schrufer TL, Bronson SK, Kimball SR, Jefferson LS. Hyperglycemia-induced O-GlcNAcylation and truncation of 4E-BP1 protein in liver of a mouse model of type 1 diabetes. *J Biol Chem* 2011;286:34286–34297
- Liu K, Paterson AJ, Chin E, Kudlow JE. Glucose stimulates protein modification by O-linked GlcNAc in pancreatic beta cells: linkage of O-linked GlcNAc to beta cell death. *Proc Natl Acad Sci USA* 2000;97:2820–2825
- Issad T, Masson E, Pagesy P. O-GlcNAc modification, insulin signaling and diabetic complications. *Diabetes Metab* 2010;36:423–435
- Duverger E, Roche AC, Monsigny M. N-acetylglucosamine-dependent nuclear import of neoglycoproteins. *Glycobiology* 1996;6:381–386
- Roos MD, Su K, Baker JR, Kudlow JE. O glycosylation of an Sp1-derived peptide blocks known Sp1 protein interactions. *Mol Cell Biol* 1997;17:6472–6480
- Gao Y, Miyazaki J, Hart GW. The transcription factor PDX-1 is post-translationally modified by O-linked N-acetylglucosamine and this modification is correlated with its DNA binding activity and insulin secretion in min6 beta-cells. *Arch Biochem Biophys* 2003;415:155–163
- Soesanto YA, Luo B, Jones D, et al. Regulation of Akt signaling by O-GlcNAc in euglycemia. *Am J Physiol Endocrinol Metab* 2008;295:E974–E980
- Han I, Kudlow JE. Reduced O glycosylation of Sp1 is associated with increased proteasome susceptibility. *Mol Cell Biol* 1997;17:2550–2558
- Zeidan Q, Hart GW. The intersections between O-GlcNAcylation and phosphorylation: implications for multiple signaling pathways. *J Cell Sci* 2010;123:13–22
- Yang X, Ongusaha PP, Miles PD, et al. Phosphoinositide signalling links O-GlcNAc transferase to insulin resistance. *Nature* 2008;451:964–969
- Griffith LS, Schmitz B. O-linked N-acetylglucosamine levels in cerebellar neurons respond reciprocally to perturbations of phosphorylation. *Eur J Biochem* 1999;262:824–831
- Cheng X, Cole RN, Zaia J, Hart GW. Alternative O-glycosylation/O-phosphorylation of the murine estrogen receptor beta. *Biochemistry* 2000;39:11609–11620
- Zeidan Q, Wang Z, De Maio A, Hart GW. O-GlcNAc cycling enzymes associate with the translational machinery and modify core ribosomal proteins. *Mol Biol Cell* 2010;21:1922–1936
- Créancier L, Morello D, Mercier P, Prats AC. Fibroblast growth factor 2 internal ribosome entry site (IRES) activity ex vivo and in transgenic mice reveals a stringent tissue-specific regulation. *J Cell Biol* 2000;150:275–281
- Le Bacquer O, Petroulakis E, Pagliarunga S, et al. Elevated sensitivity to diet-induced obesity and insulin resistance in mice lacking 4E-BP1 and 4E-BP2. *J Clin Invest* 2007;117:387–396
- Wiśniewski JR, Zougman A, Nagaraj N, Mann M. Universal sample preparation method for proteome analysis. *Nat Methods* 2009;6:359–362
- Moon MS, McDevitt EI, Zhu J, et al. Elevated hepatic iron activates NF-E2-related factor 2-regulated pathway in a dietary iron overload mouse model. *Toxicol Sci* 2012;129:74–85
- Giardina BJ, Stanley BA, Chiang HL. Comparative Proteomic Analysis of Transition of *Saccharomyces cerevisiae* from Glucose-Deficient Medium to Glucose-Rich Medium. *Proteome Sci* 2012;10:40
- Tang WH, Shilov IV, Seymour SL. Nonlinear fitting method for determining local false discovery rates from decoy database searches. *J Proteome Res* 2008;7:3661–3667
- Teshima-Kondo S, Kondo K, Prado-Lourenco L, et al. Hyperglycemia up-regulates translation of the fibroblast growth factor 2 mRNA in mouse aorta via internal ribosome entry site. *FASEB J* 2004;18:1583–1585
- Oulianova N, Falk S, Berteloot A. Two-step mechanism of phlorizin binding to the SGLT1 protein in the kidney. *J Membr Biol* 2001;179:223–242
- Yuzwa SA, Macauley MS, Heinonen JE, et al. A potent mechanism-inspired O-GlcNAcase inhibitor that blocks phosphorylation of tau in vivo. *Nat Chem Biol* 2008;4:483–490
- Komar AA, Mazumder B, Merrick WC. A new framework for understanding IRES-mediated translation. *Gene* 2012;502:75–86
- Komar AA, Hatzoglou M. Internal ribosome entry sites in cellular mRNAs: mystery of their existence. *J Biol Chem* 2005;280:23425–23428
- Schwanhäusser B, Busse D, Li N, et al. Global quantification of mammalian gene expression control. *Nature* 2011;473:337–342
- Mokrejs M, Vopálenký V, Kolenaty O, et al. IRESite: the database of experimentally verified IRES structures (www.iresite.org). *Nucleic Acids Res* 2006;34:D125–D130
- Li W, Thakor N, Xu EY, et al. An internal ribosomal entry site mediates redox-sensitive translation of Nr2f. *Nucleic Acids Res* 2010;38:778–788
- Yip CK, Murata K, Walz T, Sabatini DM, Kang SA. Structure of the human mTOR complex I and its implications for rapamycin inhibition. *Mol Cell* 2010;38:768–774
- Licursi M, Komatsu Y, Pongnopparat T, Hirasawa K. Promotion of viral internal ribosomal entry site-mediated translation under amino acid starvation. *J Gen Virol* 2012;93:951–962
- Magagnin MG, van den Beucken T, Sergeant K, et al. The mTOR target 4E-BP1 contributes to differential protein expression during normoxia and hypoxia through changes in mRNA translation efficiency. *Proteomics* 2008;8:1019–1028
- Braunstein S, Karpisheva K, Pola C, et al. A hypoxia-controlled cap-dependently translation switch in breast cancer. *Mol Cell* 2007;28:501–512
- Schrufer TL, Antonetti DA, Sonenberg N, Kimball SR, Gardner TW, Jefferson LS. Ablation of 4E-BP1/2 prevents hyperglycemia-mediated induction of VEGF expression in the rodent retina and in Muller cells in culture. *Diabetes* 2010;59:2107–2116
- Fort PE, Losiewicz MK, Reiter CE, et al. Differential roles of hyperglycemia and hypoinsulinemia in diabetes induced retinal cell death: evidence for retinal insulin resistance. *PLoS ONE* 2011;6:e26498
- Holcik M. Targeting translation for treatment of cancer—a novel role for IRES? *Curr Cancer Drug Targets* 2004;4:299–311
- Kozak M. Influences of mRNA secondary structure on initiation by eukaryotic ribosomes. *Proc Natl Acad Sci USA* 1986;83:2850–2854